

Article

Compact Design Method for Planar Antennas with Defected Ground Structures

Won Jun Lee ¹, Won-Sang Yoon ², Dal Ahn ¹  and Sang-Min Han ^{1,*} 

¹ Department of ICT Convergence, Soonchunhyang University, Asan 31538, Chungnam, Republic of Korea; xp3589@naver.com (W.J.L.); dahnkr@sch.ac.kr (D.A.)

² Department of Electronic Engineering, Hoseo University, Asan 31499, Chungnam, Republic of Korea; wsyoon@hoseo.edu

* Correspondence: smhan@sch.ac.kr

Abstract: In this paper, a compact antenna design method is proposed for microstrip patch antennas using a double-layered defected ground structure (DGS) configuration. While a conventional single-layered defected ground structure yields a lower resonant frequency and Q-factor, a smaller circuit size can be achieved using an additional substrate with a higher dielectric constant. The size reduction obtained from the additional resonant LC elements is analytically explained using the equivalent circuit model. The characteristics of the additional substrates are investigated for various dielectric constants and thicknesses. From the experimental results, the proposed design method leads to a total size reduction of up to 51.7% and a miniaturized design for planar antennas with ground apertures. The proposed design method can be applied to various antenna designs with any DGS pattern. Furthermore, the size reduction method can maintain the structure of the resonant patch element and its radiation characteristics. Therefore, the proposed method is applicable to the design of microwave devices on microstrip-based configurations.

Keywords: defected ground structures (DGSs); dielectric substrates; microstrip antennas; minimization; multi-layer circuits



Citation: Lee, W.J.; Yoon, W.-S.; Ahn, D.; Han, S.-M. Compact Design Method for Planar Antennas with Defected Ground Structures. *Electronics* **2023**, *12*, 2226. <https://doi.org/10.3390/electronics12102226>

Academic Editors: Djuradj Budimir, Syed Muzahir Abbas and Yang Yang

Received: 19 March 2023

Revised: 10 May 2023

Accepted: 11 May 2023

Published: 14 May 2023



Copyright: © 2023 by the authors. Licensee MDPI, Basel, Switzerland. This article is an open access article distributed under the terms and conditions of the Creative Commons Attribution (CC BY) license (<https://creativecommons.org/licenses/by/4.0/>).

1. Introduction

Mobile devices have been rapidly developed toward minimization and integration in order to converge various wireless systems. Whereas active front-end circuits can be integrated on a single die with a one-chip solution, microwave devices are still limited in their compactness due to the wavelength-dependent design of the resonant circuits, such as filters, duplexers, and antennas. Since a microstrip patch antenna is one of the representative planar resonant antennas designed to be integrated into mobile systems, its miniaturization has been researched using various approaches [1,2].

The defected ground structure (DGS) was invented for microstrip resonators [3] and is implemented on a ground plane to replace microstrip line resonators. Its versatile usages include effective wavelength reduction [4–7], current flow control, signal isolation, and so on. In addition, the defected patterns are directly mounted on the backsides of microstrip antenna resonators. Despite the advantages of the DGS transmission line, it is hard to implement due to the floating DGS ground plane. The electromagnetic field is fringed with the DGS aperture on a ground plane, which causes radiation loss. In general, microwave devices with DGSs need to be implemented with some air space on the ground side to avoid interferences from other materials. When a conducting material makes contact with or approaches the DGS aperture, the original characteristics of the DGS transmission line cannot be retained due to field reflections or impedance changes. Therefore, microwave devices using DGS transmission lines have been implemented only as stand-alone modules with limited multiple and composite designs [8]. Since the DGS is a resonator itself, it is difficult to analytically design a resonant antenna, because the double resonators of an

antenna and a DGS lead to unexpected resonance effects. Therefore, the applications of DGSs to antenna designs are limited in features such as compactness [1,2], polarization control [9–11], and inter-element isolation improvement [12,13]. Furthermore, the backside aperture of the DGS can contribute to bandwidth enhancement by reducing the Q-factor of the resonant antenna [14].

A microstrip patch antenna is popularly designed for a simple planar structure because it has omni-directional radiation patterns oriented toward a radiating direction. As the patch size is dependent on the resonant frequency, it requires a relatively large area on a microstrip substrate within low frequency ranges. Therefore, various modified design technologies have been researched to minimize the patch area on a planar substrate, such as patches with a shorting via pins [15,16], slots [17–21], folded patches [22,23], and fractal patch patterns [24,25]. These patch designs require specific design processes for each application because one has to modify the radiating element of the patch itself.

In this paper, a compact microstrip patch antenna with a DGS implemented on a double-layered (DL) substrate is proposed. The size reduction design procedure is introduced using an original patch antenna with a conventional single-layered (SL) DGS and a proposed DL-DGS. The double-layered substrate is designed with an SL-DGS attached to a dielectric substrate with a high dielectric constant. The suspended substrate increases the higher effective dielectric constant on the DGS surface, which can reduce the resonant antenna size. As the value of the LC increases using a DGS and an additional substrate, the resonant frequency of the antenna can be reduced because the resonant frequency is inversely proportional to the values of L and C. The proposed DL-DGS patch antenna is also modeled, verified for any additional LC resonator effects, and analyzed for its additional substrate characteristics. The proposed method can reduce the size of a planar patch antenna without any modification of the resonant patch. In addition, the patch antenna's characteristics can be maintained for the additionally attached dielectric substrate. Furthermore, the proposed design technique can be applied to any planar antenna design with ground slots to reduce the size of the radiating elements.

This paper is organized as follows. Section 2 presents the configuration of the proposed DL-DGS patch antenna and the potential to reduce the patch size. An equivalent circuit model and characterization are described for the proposed double-layered structure in Section 3. Section 4 discusses the size reduction and antenna performance based on the experimental results. In addition, a comparison with the other size reduction techniques for microstrip patch antennas with defected ground structures is provided. Finally, the feasibility and applications of the new DL-DGS patch antenna are outlined in Conclusions.

2. Double-Layered Design for Planar Patch Antennas with DGSs

A DL-DGS microstrip patch antenna with an H-shaped DGS was designed as shown in Figure 1a. The antenna pattern in the top layer and the DGS pattern in the middle layer are shown in Figure 1b. The original patch was designed without a DGS on an upper substrate, while the SL-DGS patch was designed with a DGS on an upper substrate, which is the same as the structure of the conventional DGS antenna. The proposed DL-DGS patch was configured with an additional lower substrate beneath the SL-DGS patch. For a convenient comparison of the resonator size, a microstrip square patch was designed with a resonant frequency of 2.4 GHz with $l = 41$ mm. An impedance transformer was designed with a quarter wavelength of $j = 22.8$ mm and a 135Ω width of $m = 0.3$ mm. The middle layer has a ground plane with an H-shaped DGS pattern with $a = 20$ mm, $b = 14$ mm, $c = 1$ mm, and $d = 7$ mm. The bottom layer has no metal plane. The two-layered substrate has an upper substrate with $\epsilon_{r_1} = 2.2$ and $t_1 = 31$ Mils, and the lower substrate has $\epsilon_{r_2} = 10.2$ and $t_2 = 50$ Mils. The DGS pattern determines the additional L and C values of the resonator and the effect of the lower substrate. Since the H-shaped DGS pattern has a dominant inductance, a capacitance variance corresponding to the lower substrate material is expected.

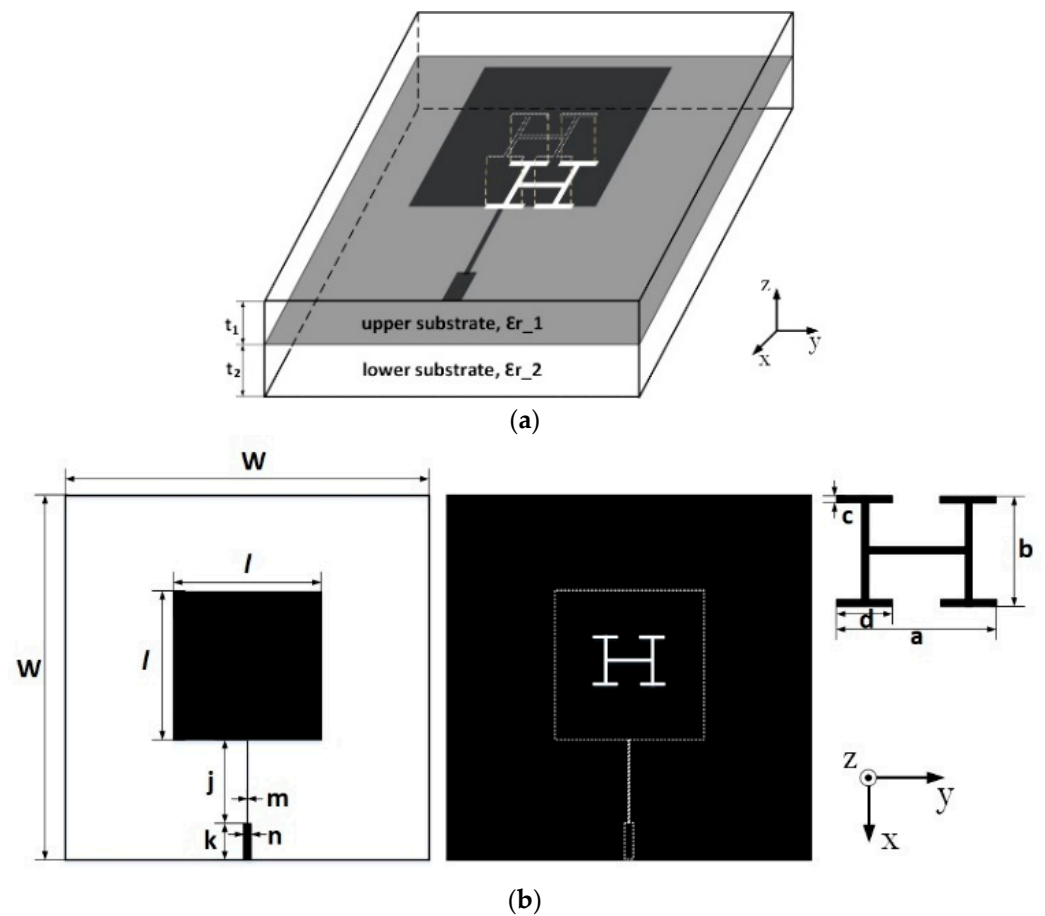


Figure 1. Configuration of the proposed DL-DGS microstrip patch antenna. (a) Double-layered configuration. (b) A top-layer view and a middle-layer view.

The effects of the DGS and additional substrate on the antenna size reduction were evaluated using an EM simulator from ANSYS HFSS (High-Frequency Structure Simulator). Figure 2 presents the S_{11} of an original, an SL-DGS, and a DL-DGS microstrip patch antenna. The original patch antenna was simulated without a DGS and a lower substrate, while the SL-DGS and DL-DGS patch antennas were simulated with an H-shaped DGS and an additional lower substrate, respectively. The original patch antenna has a resonant frequency (f_r) of 2.403 GHz, while the SL-DGS patch antenna has an f_r of 1.833 GHz. Through the DGS effect, the size of the patch antenna can be effectively reduced by 42.4%. Due to the small aperture size of the DGS, the two antennas show almost the same bandwidth. The DL-DGS microstrip patch antenna has an f_r of 1.661 GHz. The lower substrate yields an additional size reduction of the patch antenna by 10.9%. Compared to the original patch antenna, the proposed DL-DGS patch antenna is expected to achieve a size reduction of 53.3%.

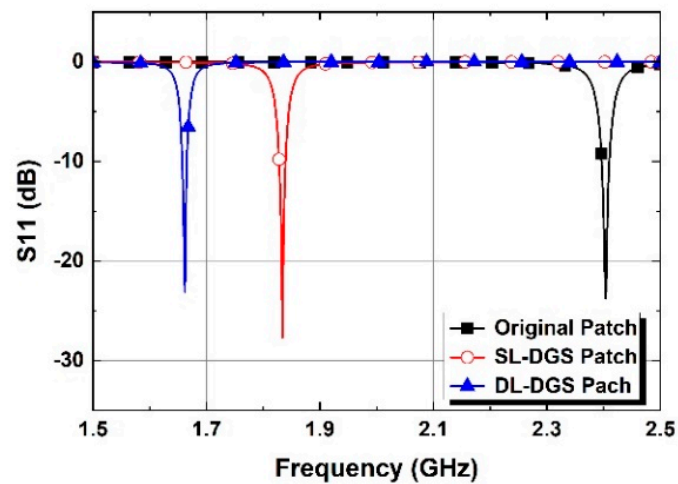


Figure 2. Simulated S11 for an original, an SL-DGS, and a DL-DGS patch antenna.

3. Design and Analysis of the Double-Layered DGS Patch Antenna

The proposed double-layer design of the microstrip patch antenna was analyzed for resonant operations using an equivalent circuit model. Figure 3 shows the equivalent circuit of the DL-DGS patch antenna. Each patch antenna design model is separately shown for the original, SL-DGS, and DL-DGS patch antennas, respectively. The original patch is modeled using an open-circuit half-wave transmission line model [26,27], while the SL-DGS antenna is modeled based on the original patch model, adding a DGS resonator of a parallel-connected L_s and C_s [8,27]. The DL-DGS antenna is modeled with an additional series-connected L_d and C_d [8].

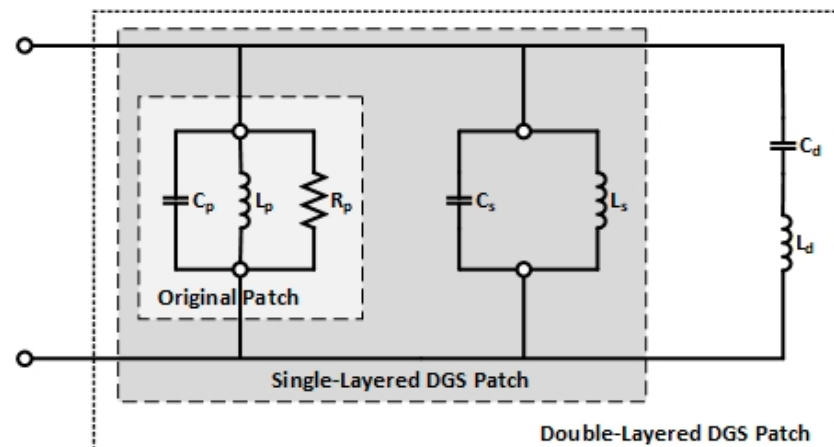


Figure 3. Equivalent circuit model of the proposed DL-DGS microstrip patch antenna.

In light of the equivalent circuit of the DL-DGS transmission line with a dumbbell-shaped DGS [8], the equivalent circuit of the DL-DGS antenna has a reasonable configuration. The equivalent circuit of the DL-DGS transmission line consists of a DGS resonator of C_s and L_s and lower substrate elements of C_d and L_d . The radiation loss parameters of R_s and R_d in the DL-DGS transmission line are ignored for an antenna equivalent circuit because the antenna itself has a radiation function. Whereas the parallel RLC resonator comprises a conventional SL-DGS model of L_s and C_s , the proposed structure has another series-resonant circuit induced by an additional ground current path. The parasitic parameters from the lower substrate of L_d and C_d account for the effect on the resonant frequency shift and Q-factor improvement because the total inductance decreases and the total capacitance increases after attaching a lower substrate. In the case of the equivalent

circuit of the DL-DGS antenna, a resonant circuit of C_p , L_p , and R_p is added as an original patch function.

In order to verify the equivalent model and characterize the effect of the additional substrate applied to the DL-DGS patch antenna, various dielectric constants of the lower substrate were applied. Figure 4A presents the resonant frequency variation in the dielectric constant of the lower substrate with a thickness of 50 Mils. To verify the effect of the double-layered structure, an SL-DGS patch antenna was compared in the case of $\epsilon_{r,2} = 1$ (air). As the dielectric constant increases from 1 to 10.2, the resonant frequency decreases from 1.833 GHz to 1.661 GHz. The solid lines show the EM simulated results, while the dashed lines present the circuit simulated results based on the equivalent circuit models. The circuit simulations were performed using an ADS (Advanced Design System) from Keysight Technologies, Ltd. The equivalent circuit models are well-matched with every substrate environment together with the EM simulated results. For the effect of the thickness of the lower substrate, resonant frequency variations were applied. Figure 4B shows the resonant frequency variations for various thicknesses with a dielectric constant of the lower substrate of 10.2. As the thickness increases from 0 Mil to 50 Mils, the resonant frequency decreases from 1.883 GHz to 1.661 GHz, which indicates an effective size reduction. A thickness of 0 Mil indicates that there is no lower substrate (SL-DGS) as a reference antenna.

The equivalent circuit elements were extracted by matching the EM simulated results with the specified antenna structure and substrate material environment. The original patch antenna model was designed with $L_p = 0.03$ nH, $C_p = 146.1$ pF, and $R_p = 57.0 \Omega$, as shown in Figure 3. Then, the resonant elements of the SL-DGS were designed with $L_s = 1.46$ nH and $C_s = 110.0$ pF.

For the various characteristics of lower substrates, the additional elements of the DL-DGS of L_d and C_d are presented in Table 1. The inductances yielded by the lower substrates are found to have almost the same value as $L_d = 0.03$ nH, whereas the capacitances increase as the dielectric constant increases. The H-shaped DGS has a relatively large inductance and small aperture size, and the material characteristics affect the additional capacitance increments. In addition, the capacitances increase as the lower substrate thickness increases.

Table 1. Characteristics of the DL-DGS patch antennas for various dielectric constants and thicknesses of the lower substrate.

$\epsilon_{r,2}$	L_d (nH)	C_d (pF)	f_r (GHz)	BW (MHz)	Q-Factor
1.0 (air)	0.00	0.00	1.833	10.9	168.2
2.0	0.03	8.24	1.803	9.7	185.8
4.0	0.03	17.7	1.770	9.3	190.3
6.0	0.03	27.5	1.734	8.7	199.3
8.0	0.03	37.2	1.699	8.2	207.1
10.2	0.03	47.6	1.661	8.0	207.7
Thickness (Mils)	L_d (nH)	C_d (pF)	f_r (GHz)	BW (MHz)	Q-factor
0 (air)	0.00	0.0	1.833	10.9	168.2
10	0.03	19.4	1.765	9.8	180.1
20	0.03	32.0	1.718	9.0	190.9
30	0.03	38.5	1.695	8.6	197.1
40	0.03	43.9	1.674	8.2	204.2
50	0.03	47.6	1.661	8.0	207.7

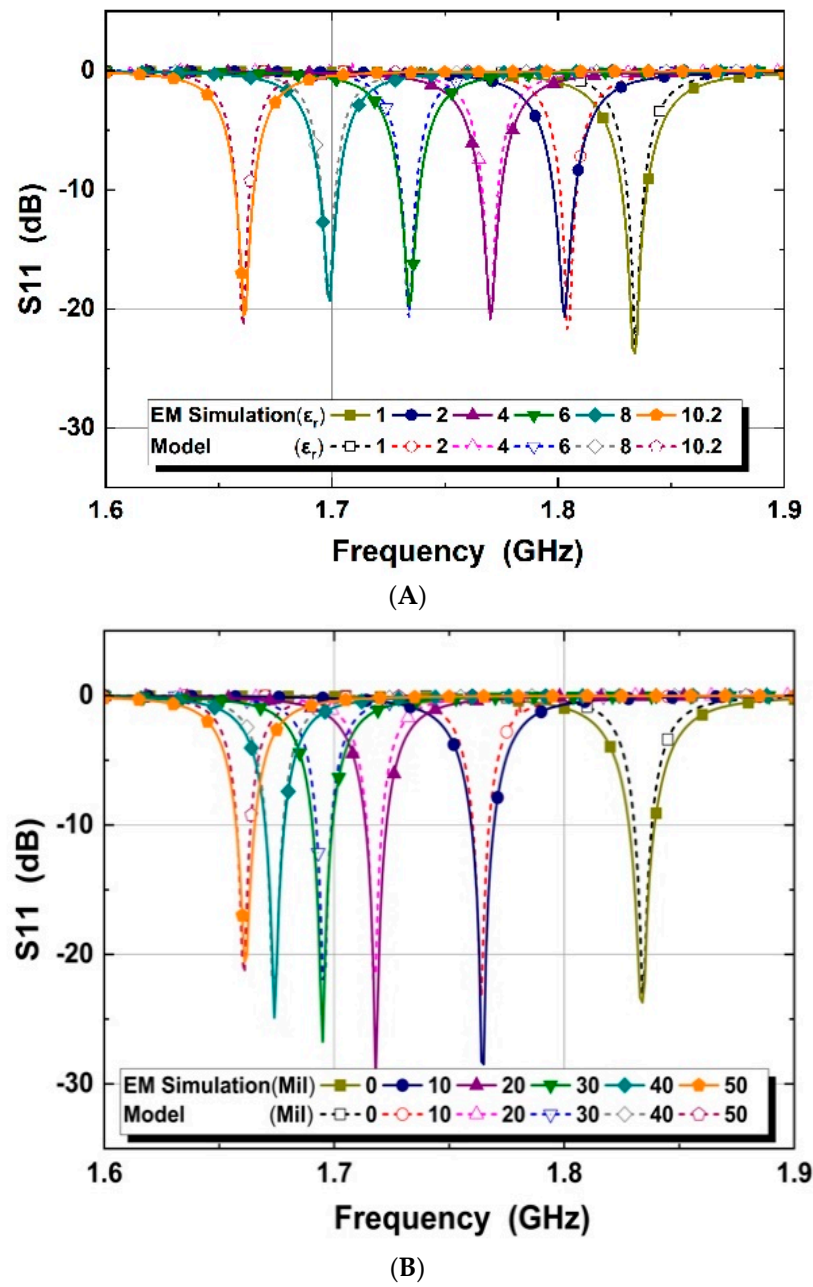


Figure 4. Resonant frequencies of the DL-DGS antenna with a lower substrate. (A) Dielectric constant variations for $t_2 = 50$ Mils. (B) Thickness variations for $\epsilon_{r_2} = 10.2$.

Table 1 summarizes the characterization of the DL-DGS patch antenna. As the dielectric constant of the attached lower substrate increases, the total amount of LC products increase; therefore, the resonant frequency is decreased. From the equivalent circuit analysis, as shown in Figure 3, the proposed structure presents as a parallel resonator model. As the general resonator model of the patch antenna of C_p , L_p , and R_p expands with another resonant circuit of C_d and L_d due to the H-shaped DGS resonator, the total capacitance increases with $C_p + C_d$. In addition, the total inductance decreases with $L_p // L_d$. When the additional lower substrate is attached, the additional series-resonant elements of C_d and L_d contribute to the additional capacitance increment and inductance decrement. Because the

equivalent circuit model of the proposed DL-DGS patch antenna has a parallel resonator model, the Q-factor can be expressed as follows:

$$Q = \frac{R}{\omega_r L} = \omega_r RC \quad (1)$$

where $\omega_r = 2\pi f_r$ and f_r indicate a resonant frequency. Therefore, the total capacitance increases and the total inductance decreases, as designed from an original patch to create the SL-DGS and DL-DGS patches, which means that the Q-factor can be increased. According to Table 1, the DL-DGS patch has a higher Q-factor than the SL-DGS patch antenna for $\epsilon_{r,2} = 1$. Additionally, as the dielectric constant increases in the lower substrate, the Q-factor increases, because a substrate with a higher dielectric constant generates a higher additional capacitance.

For the thickness variations, as for the dielectric constant variations, the same mechanism was investigated. The SL-DGS case shows a zero thickness of the lower substrate. The thicker dielectric substrate results in a higher parallel capacitance, which presents a lower resonant frequency and higher Q-factor, as shown in Table 1.

From the total capacitance increase, the resonant frequency of the DL-DGS patch is decreased while maintaining the physical patch size, which means that this technique can be used to design a smaller patch with the same resonant frequency. Therefore, the proposed method of adhering a dielectric slab with a higher dielectric constant and a greater thickness is verified.

4. Experiments and Evaluations of the Proposed Compact DL-DGS Patch Antenna

The proposed DL-DGS microstrip patch antenna was implemented on the upper substrate of an RT Duroid 5880 with $\epsilon_{r,1} = 2.2$ and $t_1 = 31$ Mils and on the lower substrate of an RT Duroid 6010 with $\epsilon_{r,2} = 10.2$ and $t_2 = 50$ Mils. Figure 5 shows photographs of the implemented DL-DGS antenna. While Figure 5a shows the top layer of the original patch on the upper substrate, the backside ground plane with an H-shaped DGS pattern on the upper substrate is presented in Figure 5b. Figure 5c shows the photo of the lower substrate without any metal on either side that is adhered to the bottom surface of the upper substrate, as shown in Figure 5b. The implemented substrate size is $W \times W = 95 \text{ mm} \times 95 \text{ mm}$.

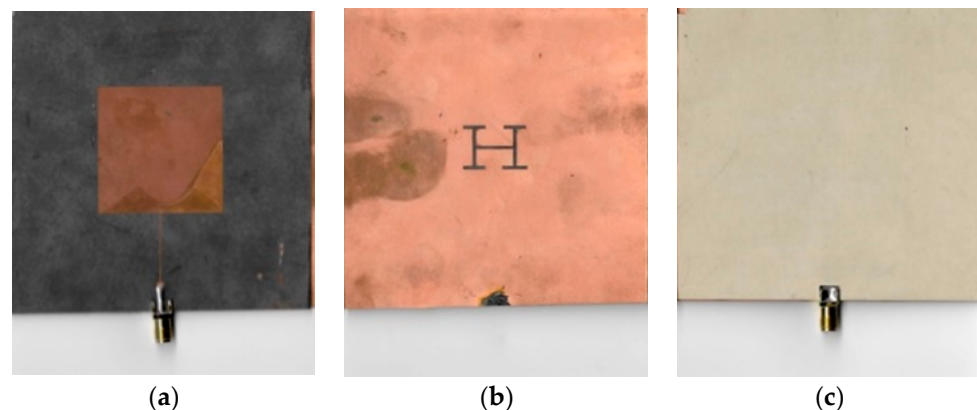


Figure 5. Photographs of the DL-DGS microstrip patch antenna. (a) Top view. (b) Middle-layer view. (c) Bottom view.

The resonant frequencies and Q-factors were measured as shown in Figure 6. The original, SL-DGS, and DL-DGS patch antennas present measured resonant frequencies of $f_r = 2.399$ GHz, 1.801 GHz, and 1.69 GHz, respectively, while the simulated results show values of 2.404 GHz, 1.834 GHz, and 1.662 GHz, respectively. The Q-factor is decreased from 243.5 for the original patch to 133.4 for the SL-DGS patch by the DGS aperture and then slightly increased to 149.5 for the DL-DGS patch after attaching a high-dielectric slab to the aperture.

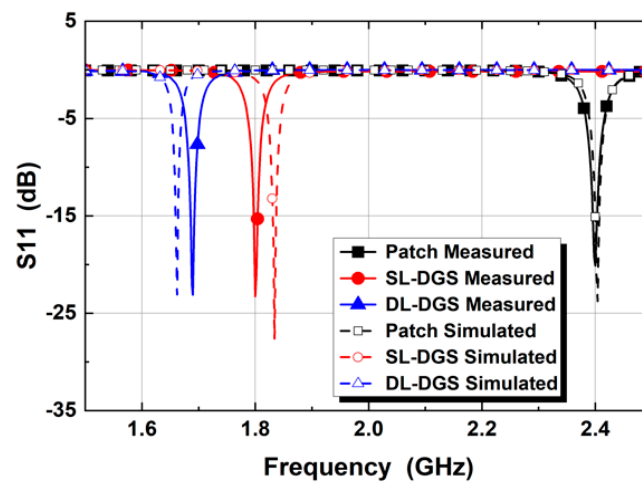


Figure 6. Measured and simulated S11 of an original patch, a conventional SL-DGS patch, and the proposed DL-DGS patch.

To compare the radiation characteristics, the antenna radiation patterns were measured in an anechoic chamber. In general, DGS antennas show a relatively poor linear polarization performance due to current direction changes induced by ground deflection. In addition, the amount of backside radiation through the DGS aperture needs to be checked before application to normal patch antennas, because the electromagnetic energy may radiate through the DGS aperture. Figure 7a,b presents the radiation patterns of the SL-DGS and DL-DGS patch antennas, respectively. Each pattern was measured for an E-plane (x - z plane) and an H-plane (y - z plane) and compared to a cross-polarization pattern. While the SL-DGS patch antenna presents a gain of 3.9 dBi, an HPBW of 68.0° , and a cross-pol. Level of -27.6 dB, the DL-DGS patch antenna shows a gain of 2.4 dBi, an HPBW of 92.0° , and a cross-pol. Level of -24.1 dB. Regarding the effect of the DGS aperture radiation, the proposed DL-DGS patch antenna maintains good linear polarization characteristics for the defected ground. Because the high-dielectric substrate absorbs the electromagnetic field toward the backside substrate of the antenna, the front-to-back ratio (F/B) of 7.3 dB for the SL-DGS antenna decreases to 4.5 dB for the DL-DGS antenna. As the dielectric material ($\epsilon_r > 1$) attracts the electromagnetic field, the additional high-dielectric substrate absorbs the backward field, which reduces the F/B compared to the SL-DGS antenna with an air backside boundary ($\epsilon_r = 1$).

Based on the proposed compact design method, the circuit size reductions were compared. At first, the original patch antenna was designed with 2.4 GHz using a basic design theory stipulating that the square patch is designed with $1 \times 1 = 0.49\lambda / \sqrt{\epsilon_r} \times 0.49\lambda / \sqrt{\epsilon_r}$ at the resonant frequency, with the expected patch size of 1681 mm^2 . The design results show a resonant frequency of 2.399 GHz with a physical size of 1681 mm^2 . With the same physical patch size, the SL-DGS patch was designed. The SL-DGS patch operates at 1.801 GHz, which should require the expected original patch size of 3025 mm^2 . Therefore, the patch antenna operating at 1.801 GHz is designed with a size of 1681 mm^2 instead of 3025 mm^2 , with a size ratio of 55.6%. The DL-DGS patch antenna operating at 1.690 GHz can be designed with a physical size of 1681 mm^2 , instead of the expected original patch size of 3481 mm^2 , with a size ratio of 48.3%. Therefore, the antenna sizes can be compared as shown in Table 2. The conventional SL-DGS patch antenna can reduce the antenna size by 44.4%, while the DL-DGS patch can reduce the antenna size by 51.7%.

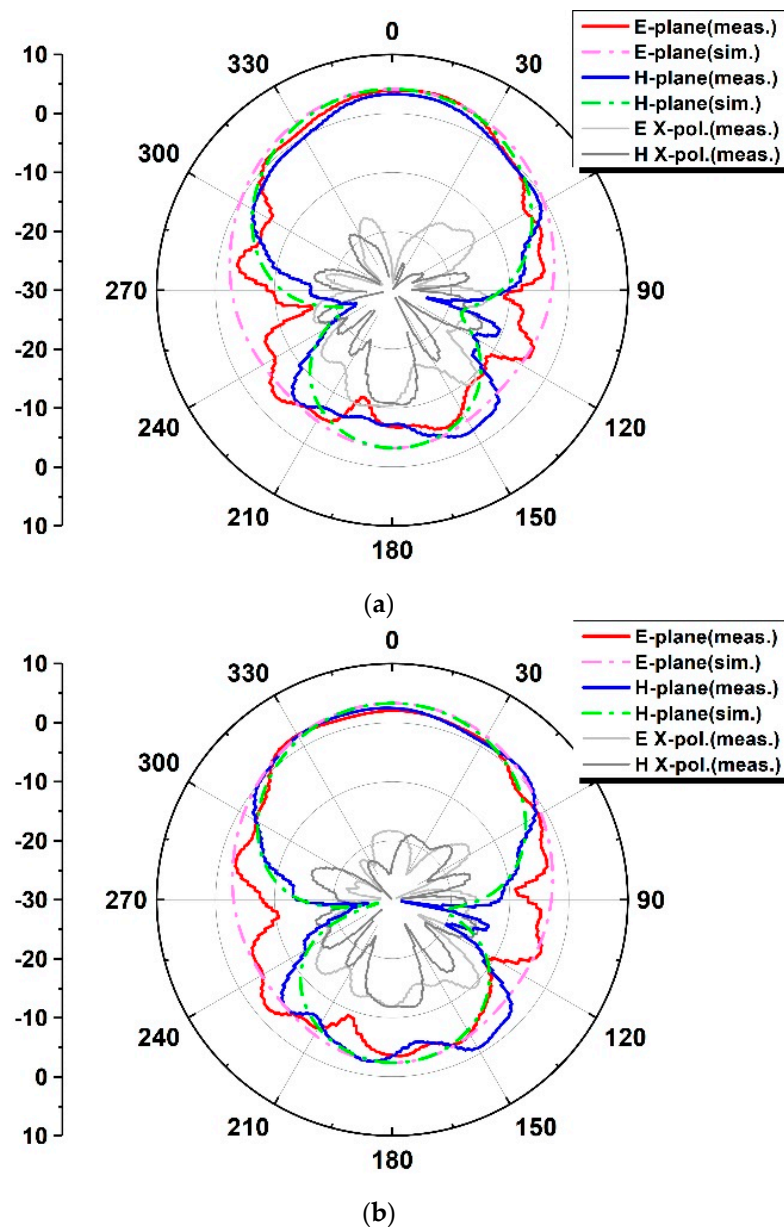


Figure 7. Measured and simulated radiation patterns. (a) SL-DGS patch antenna. (b) DL-DGS patch antenna.

Table 2. Comparison of the original, SL-DGS, and DL-DGS patch antennas.

Antenna	f_r (GHz)	Expected Original Patch Size at f_r (a, mm ²)	Physical Patch Size (b, mm ²)	Comparison (b/a × 100)
Original Patch	2.399	1681	1681	100
SL-DGS Patch	1.801	3025	1681	55.6
DL-DGS Patch	1.690	3481	1681	48.3

From the performance evaluation of the proposed size reduction methods for a planar microstrip patch antenna, it was verified that the proposed design can provide a new, additional method with which to minimize the patch with any ground plane slot. The proposed DL-DGS patch antenna maintains the original resonant element and radiation characteristics, as compared to the previous studies on the modification of patches [15,16,22–25]. In par-

ticular, as compared to the patch size reductions utilizing ground plane slots among the previous works [17–21], the patch size can be further minimized using the proposed method.

Even though it is difficult to compare size reductions, the previous works using ground plane slots were compared for the size reduction relative to a reference original patch antenna, as shown in Table 3. It is assumed that all the patch antennas have a patch area of $\lambda \times \lambda \text{ mm}^2$ that is the inverse of the square of resonant frequency, because each paper uses a different comparison. Because these design methods were compared for each design technique, the method in this work was compared for the SL-DGS patch, and the additional reduction method for the DL-DGS patch was appended. The paper [17] presents a coaxial-fed patch with a linear slot cross on a ground backside at 2.87 GHz. The position of the linear slot is a variable of the size reduction. The maximum rate of the size reduction is approximately 77.3%. The authors of [18] designed a planar microstrip-fed patch with meandering line slots operating at 5.989 GHz. The patch with an open-end slot type has an 83% maximum size reduction. The authors of [19] explored similar slot types with coaxial feeding at 2.387 GHz that has a 55.8% reduction rate, while the authors of [20] explored a cross-type array of four slots for a coaxial-fed patch operating at 2.84 GHz with a 73.2% reduction. The authors of [21] investigated a CSRR (Complementary Split-Ring Resonator)-type slot array for a microstrip patch operating at 5.0 GHz with a 42.2% reduction rate. The proposed structures of the SL-DGS and DL-DGS patch antennas were compared with those in the previous works for the reduction techniques, feeding types of the microstrip patches, resonant frequencies, and the size reduction rates. The SL-DGS patch antenna (the conventional DGS patch) is comparable to the previous works. However, the DL-DGS technique can provide additional size reductions compared to every comparable patch antenna design with defected slots on a ground plane.

Table 3. Comparison of the recent patch antenna reduction technologies with ground slots.

		Reduction Method	Feeding Type	f_r (GHz) of Ref. Antenna	Size Reduction (%)
	[17]	line slot position	coaxial	2.87	77.3
	[18]	meandering line type	planar	5.98	83.0
	[19]	meandering line offset	coaxial	2.387	55.8
	[20]	slot size	coaxial	2.84	73.2
	[21]	CSRR slot	planar	5.0	42.2
This work	SL-DGS	additional substrate	planar	2.4	44.4
	DL-DGS				51.7

5. Conclusions

A size reduction design method for microstrip patch antennas with defected ground structures was proposed using a double-layered substrate. While the size of a normal patch antenna can be reduced by designing DGS patterns on a ground plane, an additional size reduction can be achieved by attaching a lower substrate. The operating mechanism was described based on an equivalent circuit model with each LC resonant circuit for the characteristics of the additional dielectric substrate. According to the experimental results, the proposed DL-DGS patch antenna can reduce the circuit size by up to 51.7%, while the conventional SL-DGS patch antenna reduces the size by 44.4%. The proposed size reduction method can maintain the resonator structure and resonance characteristics of the original microstrip patch antenna. Therefore, as compared to the original patch antenna, almost the same radiation performance can be achieved with the small resonant radiator. Furthermore, for all the resonant antenna configurations with various DGS patterns and sizes, the proposed method can be applied to reduce the size of the planar antenna resonators. The proposed new double-layered DGS antenna design technology can be used for various efficient designs of compact and novel microwave devices.

Author Contributions: Conceptualization, S.-M.H.; methodology, W.-S.Y. and D.A.; software, W.J.L.; validation, W.J.L. and S.-M.H.; formal analysis, D.A.; investigation, W.-S.Y.; resources, W.J.L.; data curation, W.J.L.; writing—original draft preparation, W.J.L.; writing—review and editing, S.-M.H.; visualization, W.J.L.; supervision, S.-M.H.; project administration, S.-M.H.; funding acquisition, S.-M.H. and D.A. All authors have read and agreed to the published version of the manuscript.

Funding: This work was supported by “Regional Innovation Strategy (RIS)” through the National Research Foundation of Korea funded by the Ministry of Education (2021RIS-004), the MSIT, Korea, under the ICAN program (IITP-2023-2020-0-01832) supervised by the IITP, and the Soonchunhyang University research fund.

Data Availability Statement: The dataset is not applicable.

Conflicts of Interest: The authors declare no conflict of interest.

References

1. Salih, A.; Sahrawi, M.S. A dual-band highly miniaturized patch antenna. *IEEE Antennas Wirel. Propag. Lett.* **2016**, *15*, 1783–1786. [[CrossRef](#)]
2. Oulhaj, O.; Touhami, N.A.; Aghoutane, M.; Tazon, A. A miniature microstrip patch antenna array with defected ground structure. *Int. J. Microw. Opt. Technol.* **2016**, *11*, 32–39.
3. Kim, C.-S.; Park, J.-S.; Ahn, D.; Lim, J.-B. A novel 1-D periodic defected ground structure for planar circuits. *IEEE Microw. Guid. Wave Lett.* **2000**, *10*, 131–133.
4. Ting, S.-W.; Tam, K.-W.; Martins, R.P. Miniaturized microstrip lowpass filter with wide stopband using double equilateral U-shaped defected ground structure. *IEEE Microw. Wirel. Comp. Lett.* **2006**, *16*, 240–242. [[CrossRef](#)]
5. Choi, H.; Lim, J.; Jeong, Y. A new design of Doherty amplifiers using defected ground structure. *IEEE Microw. Wirel. Comp. Lett.* **2006**, *16*, 687–689. [[CrossRef](#)]
6. Jahan, N.; Rahim, S.A.E.A.; Mosalam, H.; Barakat, A.; Kaho, T.; Pokharel, R.K. 22-GHz-band oscillator using integrated H-shape defected ground structure resonator in 0.18- μm CMOS technology. *IEEE Microw. Wirel. Comp. Lett.* **2018**, *28*, 233–235. [[CrossRef](#)]
7. Woo, D.-J.; Lee, T.-K. Suppression of harmonics in Wilkinson power divider using dual-band rejection by asymmetric DGS. *IEEE Trans. Microw. Theory Tech.* **2005**, *53*, 2139–2144.
8. Han, S.-M.; Kim, J.O.; Yoon, W.-S.; Lim, J.; Ahn, D. Design and characterization of the double-layered defected ground structure transmission line with less radiation effect. *Microw. Opt. Technol. Lett.* **2019**, *61*, 903–906. [[CrossRef](#)]
9. Yoon, W.-S.; Baik, J.-W.; Lee, H.-S.; Pyo, S.; Han, S.-M.; Kim, Y.-S. A reconfigurable circularly polarized microstrip antenna with a slotted ground plane. *IEEE Antennas Wirel. Propag. Lett.* **2010**, *9*, 1161–1164. [[CrossRef](#)]
10. Thakur, J.P.; Park, J. An advance design approach for circular polarization of the microstrip antenna with unbalance DGS feedlines. *IEEE Antennas Wirel. Propag. Lett.* **2006**, *5*, 101–103. [[CrossRef](#)]
11. Lee, S.-J.; Lee, H.; Yoon, W.-S.; Park, S.-J.; Lim, J.; Ahn, D.; Han, S.-M. Circular polarized antenna with controlled current distribution by defected ground structures. In Proceedings of the 2010 International Symposium on Antennas and Propagation (ISAP 2010), Macau, China, 23–26 November 2010.
12. Luo, C.; Hong, J.; Zhong, L. Isolation enhancement of a very compact UWB-MIMO slot antenna with two defected ground structures. *IEEE Antennas Wirel. Propag. Lett.* **2015**, *14*, 1766–1769. [[CrossRef](#)]
13. Sharawi, M.S.; Numan, A.B.; Khan, M.U.; Aloï, D.N. A dual-element dual-band MIMO antenna system with enhanced isolation for mobile terminals. *IEEE Antennas Wirel. Propag. Lett.* **2012**, *11*, 1006–1009. [[CrossRef](#)]
14. Zeng, J.; Luk, K. A simple wideband magnetoelectric dipole antenna with a defected ground structure. *IEEE Antennas Wirel. Propag. Lett.* **2018**, *17*, 1497–1500. [[CrossRef](#)]
15. Chen, I.-F.; Peng, C.-M. A novel reduced-size edge-shortened patch antenna for UHF band applications. *IEEE Antennas Wirel. Propag. Lett.* **2009**, *8*, 475–477. [[CrossRef](#)]
16. Wu, D.-L.; Chen, J.H.; Yang, K.Y.; Zhu, W.J.; Ye, L.H. A compact dual-polarized patch antenna with L-shaped short pins. *IEEE Antennas Wirel. Propag. Lett.* **2023**, *22*, 689–693. [[CrossRef](#)]
17. Sarkar, S.; Majumdar, A.D.; Mondal, S.; Biswas, S.; Sarkar, D.; Sarkar, P.P. Miniaturization of rectangular microstrip patch antenna using optimized single-slotted ground plane. *Microw. Opt. Technol. Lett.* **2011**, *53*, 111–115. [[CrossRef](#)]
18. Rabhakar, H.V.; Kummuri, U.K.; Yadahalli, R.M.; Munnappa, V. Effect of various meandering slots in rectangular microstrip antenna ground plane for compact broadband operation. *Electron. Lett.* **2007**, *43*, 16–17.
19. Kuo, J.-S.; Wong, K.-I. A compact microstrip antenna with meandering slots in the ground plane. *Microw. Opt. Technol. Lett.* **2001**, *29*, 95–97. [[CrossRef](#)]
20. Lin, S.-Y.; Huang, K.-C. A compact microstrip antenna for GPS and SCS application. *IEEE Trans. Antennas Propag.* **2005**, *53*, 1227–1229.
21. Jang, H.A.; Kim, D.O.; Kim, C.Y. Size reduction of patch antenna array using CSRRs loaded ground plane. In Proceedings of the Progress in Electromagnetics Research Symposium, Kuala Lumpur, Malaysia, 27–30 March 2012; pp. 1487–1489.

22. Li, Y.; Podilchak, S.K.; Anagnostou, D.E.; Constantinides, C.; Walkinshaw, T. Compact antenna for picosatellites using a meandered folded-shortened patch array. *IEEE Antennas Wirel. Propag. Lett.* **2020**, *19*, 477–481. [[CrossRef](#)]
23. Lau, K.L.; Kong, K.C.; Luk, K.M. A miniature folded shortened patch antenna for dual-band operation. *IEEE Trans. Antennas Propag.* **2007**, *55*, 2391–2398. [[CrossRef](#)]
24. Chen, W.-L.; Wang, G.-M.; Zhang, C.-X. Small-size microstrip patch antennas combining Koch and Sierpinski fractal-shapes. *IEEE Antennas Wirel. Propag. Lett.* **2008**, *7*, 738–741. [[CrossRef](#)]
25. Amini, A.; Oraizi, H.; Chaychizadeh, M.A. Miniaturized UWB log-periodic square fractal antenna. *IEEE Antennas Wirel. Propag. Lett.* **2015**, *14*, 1322–1325. [[CrossRef](#)]
26. Melkeri, V.S.; Mallikarjun, S.L.; Hunagund, P.V. H-shape defected ground structure embedded square patch antenna. *Int. J. Adv. Res. Eng. Technol.* **2015**, *6*, 73–79.
27. Woo, D.-J.; Lee, T.-K.; Lee, J.W. Equivalent circuit model for a simple slot-shaped DGS microstrip line. *IEEE Microw. Wirel. Comp. Lett.* **2013**, *23*, 447–449. [[CrossRef](#)]

Disclaimer/Publisher’s Note: The statements, opinions and data contained in all publications are solely those of the individual author(s) and contributor(s) and not of MDPI and/or the editor(s). MDPI and/or the editor(s) disclaim responsibility for any injury to people or property resulting from any ideas, methods, instructions or products referred to in the content.